

Rare decays $B \rightarrow X_s \tau^+ \tau^-$ and $B_s \rightarrow \tau^+ \tau^- \gamma$ in technicolor with scalars

Zhaohua Xiong ^{a,b,c} and Jin Min Yang ^b

^a CCAST (World Laboratory), P.O.Box 8730, Beijing 100080, China

^b Institute of Theoretical Physics, Academia Sinica, Beijing 100080, China

^c Institute of High Energy Physics, Academia Sinica, Beijing 100039, China

(December 2, 2024)

We examined the rare decays $B \rightarrow X_s \tau^+ \tau^-$ and $B_s \rightarrow \tau^+ \tau^- \gamma$ in the framework of technicolor with scalars. The contributions from the neutral and charged scalars, predicted in such technicolor model, are found to significantly enhance the branching ratio and the forward-backward asymmetry of these decays. While the contributions to $B \rightarrow X_s \tau^+ \tau^-$ arise dominantly from the charged scalars, for $B_s \rightarrow \tau^+ \tau^- \gamma$ the effects of the neutral scalars could also be sizable in some part of parameter space. These large effects might be observable in the B-factories.

12.60.NZ, 13.25.Hw

Key words: technicolor with scalars decay $B \rightarrow X_s \tau^+ \tau^-$ decay $B_s \rightarrow \tau^+ \tau^- \gamma$ forward-backward asymmetry

I. INTRODUCTION

One intriguing puzzle in particle physics is the regular pattern of the three lepton and quark families. The existence of families gives rise to many parameters of the standard model (SM). Flavor changing neutral currents (FCNC) induced B-meson rare decays provide an ideal opportunity for extracting information about the fundamental parameters of the SM, such as the Cabibbo-Kobayashi-Maskawa (CKM) matrix elements, and for testing the SM predictions at loop level and probing possible new physics. The experimental discovery of the inclusive and exclusive rare decays $b \rightarrow X_s \gamma$ and $B \rightarrow K \gamma$ [1] stimulated the study of radiative rare B-meson decays with a new momentum.

The inclusive decays $B \rightarrow X_s \ell^+ \ell^-$ ($\ell = e, \mu$) have been well studied in the frameworks of minimal supersymmetric model [2], the two Higgs doublet model(2HDM) [3–5] and the technicolor models [6,7]. It was shown that the matrix elements are strong suppressed by a factor m_ℓ/m_W and the contributions from exchanging neutral scalars can be safely neglected. However, the situation is different in the case of $\ell = \tau$. The branching ratio $Br(B_s \rightarrow \tau^+ \tau^-) \simeq 8 \times 10^{-7}$ [8] in the SM is large enough to be observable in future B-factories. The contributions from neutral scalars exchange to $B \rightarrow X_s \tau^+ \tau^-$ may no longer be negligible and thus have to be examined.

On the other hand, among rare B-meson decays, $B_s \rightarrow \tau^+ \tau^- \gamma$ is of special interest due to its relative cleanliness and sensitivity to models beyond the SM [9,10]. We emphasize that when photon is emitted in addition to the lepton pair, no helicity suppression exists, and “large” branching ratio is expected. As in the decay of $B_s \rightarrow \tau^+ \tau^-$, we could expect that for $B_s \rightarrow \tau^+ \tau^- \gamma$ the contributions from exchanging neutral scalars could also be sizable.

In this work, we will calculate the branching ratios for the inclusive and exclusive decays $B \rightarrow X_s \tau^+ \tau^-$ and $B_s \rightarrow \tau^+ \tau^- \gamma$ in technicolor model with scalar. The paper is organized as follows. Sec. II is a brief review of the model. Some detailed theoretical descriptions, especially the contributions from the neutral scalars, are presented in Sec. III and IV for the decays $B \rightarrow X_s \tau^+ \tau^-$ and $B_s \rightarrow \tau^+ \tau^- \gamma$, respectively. Finally, in Sec. V we present some numerical results and discussions.

II. TECHNICOLOR WITH SCALARS

In the technicolor model with scalars, the rare decay processes we will study receive contributions not only from the SM particles but also from charged and neutral physical scalars predicted in such a technicolor model. In this section we will briefly discuss the model and give the relevant Lagrangian which are needed in our calculation. More details of the model have been described in Refs. [11,12].

The gauge structure of the technicolor model with scalars is simply the direct product of the technicolor and standard model gauge groups: $SU(N)_{TC} \times SU(3)_C \times SU(2)_W \times U(1)_Y$ [12]. The ordinary techni-singlet fermions are exactly as those in the SM. The technicolor sector consists of two techniflavors p and m that also transform under $SU(2)_W$. In addition to the above particle spectrum, there exists a scalar doublet ϕ to which both the ordinary fermions and technifermions are coupled. Unlike the SM Higgs doublet, ϕ does not cause electroweak symmetry breaking but obtains a non-zero effective vacuum expectation value (VEV) when technicolor breaks the symmetry.

We can rewrite the matrix form of the scalar doublet $\Phi = (\tilde{\phi}\phi)$ in terms of an isosinglet scalar field σ and a unitary matrix Σ' as

$$\Phi = \begin{bmatrix} \bar{\phi}^0 & \phi^+ \\ -\phi^- & \phi^0 \end{bmatrix} \equiv \frac{(\sigma + f')}{\sqrt{2}} \Sigma', \quad (2.1)$$

where the non-linear representation $\Sigma = \exp(\frac{2i\pi}{f})$ and $\Sigma' = \exp(\frac{2i\pi}{f'})$ are adopted for the technipion fields. In this case, the kinetic terms for the scalars fields can be written as

$$\mathcal{L}_{K.E.} = \frac{1}{2} \partial_\mu \sigma \partial^\mu \sigma + \frac{1}{4} f^2 \text{Tr}(D_\mu \Sigma^\dagger D^\mu \Sigma) + \frac{1}{4} (\sigma + f')^2 \text{Tr}(D_\mu \Sigma'^\dagger D^\mu \Sigma), \quad (2.2)$$

with the covariant derivative defined by

$$D^\mu \Sigma = \partial^\mu \Sigma - ig W_a^\mu \frac{\tau^a}{2} \Sigma + ig' B^\mu \Sigma \frac{\tau^3}{2}. \quad (2.3)$$

Here τ^a ($a = 1, 2, 3$) are the SU(2) generators, W_μ^a (B_μ) denote the corresponding SU(2) (U(1)) vector fields with the gauge coupling constant g (g'). f and f' are the technipion decay constant and effective VEV, respectively. The definition of $D^\mu \Sigma'$ is analogous to that of $D^\mu \Sigma$.

The mixing will happen between π and π' . One linear combination

$$\pi_a = \frac{f\pi + f'\pi'}{\sqrt{f^2 + f'^2}} \quad (2.4)$$

becomes the longitudinal component of the W and Z, and the orthogonal linear combination

$$\pi_p = \frac{-f'\pi + f\pi'}{\sqrt{f^2 + f'^2}} \quad (2.5)$$

remains in the low-energy theory as an isotriplet of physical scalars. From Eq. (2.2) one can obtain the correct gauge boson masses providing that

$$f^2 + f'^2 = v^2 \quad (2.6)$$

with the electroweak scale $v = 246 \text{ GeV}$.

Additionally, the contributions to scalar potential generated by the technicolor interactions should be included in this model. The simplest term one can construct is

$$\mathcal{L}_T = c_1 4\pi f^3 \text{Tr} \left[\Phi \begin{pmatrix} h_+ & 0 \\ 0 & h_- \end{pmatrix} \Sigma^\dagger \right] + h.c., \quad (2.7)$$

where c_1 is a coefficient of order unity, and h_+ and h_- are the scalar's Yukawa couplings to p (h_+) and m (h_-). From Eq. (2.7) we can estimate the mass of the charged scalar at lowest order,

$$m_{\pi_p}^2 = 2\sqrt{2}(4\pi f/f')v^2 h \quad (2.8)$$

with $h = (h_+ + h_-)/2$. When the largest Coleman-Weinberg corrections for the σ field are included in the effective chiral Lagrangian [12], one obtains the constraint

$$\tilde{M}_\phi^2 f' + \frac{\tilde{\lambda}}{2} f'^3 = 8\sqrt{2}\pi c_1 h f^3 \quad (2.9)$$

and the isoscalar mass as

$$m_\sigma^2 = \tilde{M}_\phi^2 + \frac{2}{3\pi^2} [6(\frac{m_t}{f'})^4 + Nh^4] f'^2 \quad (2.10)$$

in limit (i), and

$$m_\sigma^2 = \frac{3}{2} \tilde{\lambda} f'^2 - \frac{1}{4\pi^2} [6(\frac{m_t}{f'})^4 + N h^4] f'^2 \quad (2.11)$$

in limit (ii). Here m_t is the pole mass of top quark, $\tilde{M}_\phi, \tilde{\lambda}$ are the shifted scalar mass and coupling. We will assume that $N=4$ and $c_1 = 1$ in all quantitative calculations.

In general, f and f' can depend on h_+, h_-, M_ϕ and λ , where M_ϕ is the mass of the scalar doublet ϕ , and λ is ϕ^4 coupling. Two limits of the model have been studied previously in the literatures: (i) the limit in which λ is small and can be neglected [11], and (ii) the limit in which M_ϕ is small and can be neglected [12]. The advantage of working in these two limits is that at the lowest order the phenomenology depends on h , not on the difference of h_+ and h_- , and can be described in terms of (\tilde{M}_ϕ, h) in limit (i) and $(\tilde{\lambda}, h)$ in limit (ii). In this paper, we will work in the unitary gauge, where the particle spectrum consists of π_p, σ and the massive weak gauge bosons. We choose two parameters $(f/f', m_{\pi_p})$ in both limits of the model.

The interactions relevant to our calculations can be extracted from Eq. (2.2) and Eq. (2.7). They are given by

$$\begin{aligned} \mathcal{L} = & \left(\frac{f}{f'} \right) \frac{gm_W}{2} \sigma W_\mu^+ W_\mu^- + \left(\frac{f'}{V} \right) \frac{gm_Z}{\cos \theta_W} \sigma Z^\mu Z_\mu - \left(\frac{f}{V} \right) \frac{g}{2} \sigma [W_\mu^- \partial^\mu \pi_p^+ + W_\mu^+ \partial^\mu \pi_p^-] \\ & + \left(\frac{V}{f} \right) \frac{gm_{\pi_p}^2}{2m_W} \sigma \pi_p^+ \pi_p^- + \left(\frac{V}{f'} \right) \frac{ig}{2m_W} \sigma [m_U \bar{U} U + m_D \bar{D} D] \\ & + \frac{ig}{2} \left[W_\mu^- \pi_p^+ \overset{\leftrightarrow}{\partial}^\mu \pi_p^0 + W_\mu^+ \pi_p^- \overset{\leftrightarrow}{\partial}^\mu \pi_p^0 \right] + \frac{ig \cos 2\theta_W}{2 \cos \theta_W} Z_\mu \pi_p^+ \overset{\leftrightarrow}{\partial}^\mu \pi_p^- \\ & + ie \sin \theta_W A_\mu \pi_p^+ \overset{\leftrightarrow}{\partial}^\mu \pi_p^- + \left(\frac{f}{f'} \right) \frac{ig}{2m_W} \pi_p^0 [m_U \bar{U} \gamma_5 U - m_D \bar{D} \gamma_5 D] \\ & - \left(\frac{f}{f'} \right) \frac{ig}{2\sqrt{2}} \{ \pi_p^+ \bar{U}_i [(m_U - m_D) - (m_U + m_D) \gamma_5] V_{ij} D_j \\ & - \pi_p^- \bar{D}_i V_{ij}^* [(m_U - m_D) + (m_U + m_D) \gamma_5] U_j \} \end{aligned} \quad (2.12)$$

where U, D and m_U, m_D represent the column vector and the diagonal mass matrix for the up, down-quarks respectively, π_p stands for the scalar field, and V_{ij} are the elements of the CKM matrix. The physics scalar-lepton couplings can be read off from the expression above by replacing (U, D) with the corresponding lepton fields, replacing quark mass matrices with the corresponding diagonal lepton mass matrices, and setting $V_{ij} = 1$.

III. $B \rightarrow X_s \tau^+ \tau^-$ IN TECHNICOLOR MODEL WITH SCALARS

It is well known that inclusive decay rates of heavy hadrons can be calculated in heavy quark effective theory (HQET) [13], and the leading terms in $1/m_Q$ expansion turn out to be the decay of a free heavy quark and corrections stem from the order $1/m_Q^2$ [14]. In the technicolor model with scalars, the short distance contribution to $b \rightarrow \tau^+ \tau^-$ decay can be computed in the framework of the QCD corrected effective weak Hamiltonian, obtained by integrating out heavy particles, i.e., top quark, scalar σ, π_p and W^\pm, Z bosons

$$\mathcal{H}_{eff} = \frac{4G_F}{\sqrt{2}} V_{tb} V_{ts}^* \left(\sum_{i=1}^{10} [C_i(\mu) \mathcal{O}_i(\mu) + C_{Q_i}(\mu) \mathcal{Q}_i(\mu)] \right) \quad (3.1)$$

where \mathcal{O}_i are the same as these given in Ref. [3]. The additional operators \mathcal{Q}_i [4] are due to the neutral scalars exchange diagrams, which give considerable contributions in the case that the final lepton pair is $\tau^+ \tau^-$. Here we only present the explicit expressions of the operators governing $B \rightarrow X_s \tau^+ \tau^-$. They read

$$\begin{aligned} \mathcal{O}_7 &= \frac{e}{16\pi^2} m_b (\bar{s}_\alpha \sigma^{\mu\nu} R b_\alpha) F_{\mu\nu}, \\ \mathcal{O}_8 &= \frac{e}{16\pi^2} (\bar{s}_\alpha \gamma^\mu L b_\alpha) (\bar{\tau} \gamma_\mu \tau), \\ \mathcal{O}_9 &= \frac{e}{16\pi^2} (\bar{s}_\alpha \gamma^\mu L b_\alpha) (\bar{\tau} \gamma_\mu \gamma_5 \tau), \\ \mathcal{Q}_1 &= \frac{e^2}{16\pi^2} (\bar{s}_\alpha R b_\alpha) (\bar{\tau} \gamma_\mu \tau), \\ \mathcal{Q}_2 &= \frac{e^2}{16\pi^2} (\bar{s}_\alpha R b_\alpha) (\bar{\tau} \gamma_\mu \gamma_5 \tau) \end{aligned} \quad (3.2)$$

where $L, R = (1 \mp \gamma_5)/2$, α , $F^{\mu\nu}$ are SU(3) color index and the field strength tensor of the electromagnetic interaction, respectively.

In general in theories beyond the SM there will be additional contributions, which *are characterized by the values of the coefficients C_i and C_{Q_i} at the perturbative scale m_W* . Using the Feynman rules presented in the preceding section, we can calculate the additional contributions arising from the scalars σ and π_p (π_p^0, π_p^\pm). At the scale of m_W , the Feynman diagrams for the charged scalar contributions are depicted in Fig.1, while Fig.2 shows the additional contributions from the neutral scalars. Note that the tau lepton pair is produced via exchanging γ or Z in Fig.1 and exchanging a neutral scalar σ or π_p^0 in Fig.2. The contributions to the leading order coefficients from Fig. 1 are given by [15]

$$\begin{aligned} C_7(m_W)_{TC} &= \left(\frac{f}{f'}\right)^2 H_1(x_{\pi_p}), \\ C_8(m_W)_{TC} &= \left(\frac{f}{f'}\right)^2 \frac{4 \sin^2 \theta_W - 1}{\sin^2 \theta_W} [x_W H_2(x_{\pi_p}) - x_{\pi_p} H_3(x_{\pi_p})], \\ C_9(m_W)_{TC} &= \left(\frac{f}{f'}\right)^2 \frac{x_W}{\sin^2 \theta_W} H_2(x_{\pi_p}) \end{aligned} \quad (3.3)$$

where $x_i = m_i^2/m_i^2$ and θ_W is the Weinberg angle. The functions H_i are given by

$$\begin{aligned} H_1(x) &= \frac{x}{12(x-1)^3} \left[\frac{22x^2 - 53x + 25}{6} - \frac{3x^2 - 8x + 4}{x-1} \ln x \right], \\ H_2(x) &= \frac{x}{8(x-1)} \left[-1 + \frac{1}{x-1} \ln x \right], \\ H_3(x) &= \frac{1}{18(x-1)^3} \left[\frac{47x^2 - 79x + 38}{6} - \frac{3x^3 - 6x + 4}{x-1} \ln x \right]. \end{aligned} \quad (3.4)$$

Several authors have studied decays of $b \rightarrow X_c \tau \nu$ [16], $b \rightarrow X_s \gamma$ [16,17], $Z \rightarrow b\bar{b}$ [17], $B \rightarrow X_s \mu^+ \mu^-$ [18] and $B\overline{B}$ mixing in technicolor model with scalars [11,12,17]. By comparing experimental values with the model predictions, they determined constraints on the model parameter space

$$\frac{f}{f'} \leq 0.03 \left(\frac{m_{\pi_p}}{1 \text{ GeV}}\right), \quad 95\% \text{ C. L.} \quad (3.5)$$

(see Eq. (3.5,3.6) in [16]). So for large m_{π_p} the ratio $\frac{f}{f'}$ could be large. For large f/f' , the contributions from neutral scalars exchange to $B \rightarrow X_s \tau^+ \tau^-$, as shown in Fig.2, are no longer negligible and should also be taken into account. In fact, the neutral scalar exchange diagrams (Fig.2) could give comparable contributions to those from γ , Z exchange (Fig.1) because there is an enhancement factor $(\frac{f}{f'})^4$ for the former. Since $C_i(m_W)_{TC}$ ($i = 7, 8, 9$) are proportional to $(\frac{f}{f'})^2$, and $\frac{m_\tau m_b}{m_W^2} (\frac{f}{f'})^2 \sim 1$ when $\frac{f}{f'} \geq 25$, we find that only the $O((\frac{f}{f'})^4)$ have to be included in the neutral scalar contributions to $C_{Q_j}(m_W)$ ($j = 1, 2$) so that $C_{Q_j}(m_W)$ are comparable with $C_i(m_W)$. When only $(\frac{f}{f'})^4$ dependent terms included, they can be expressed as

$$\begin{aligned} C_{Q_1}(m_W) &= -\left(\frac{f}{f'}\right)^4 \frac{m_b m_\tau}{m_\sigma^2} \frac{x_W}{4 \sin^2 \theta_W} H_4(x_{\pi_p}), \\ C_{Q_2}(m_W) &= -\left(\frac{f}{f'}\right)^4 \frac{m_b m_\tau}{m_{\pi_p}^2} \frac{x_W}{4 \sin^2 \theta_W} H_5(x_{\pi_p}) \end{aligned} \quad (3.6)$$

with

$$\begin{aligned} H_4(x) &= \frac{1}{2(x-1)^2} \left[\frac{4x^2 - 7x + 1}{2} - \frac{x^2 - 2x}{x-1} \ln x \right], \\ H_5(x) &= \frac{1}{(x-1)} \left[\frac{x+1}{2} - \frac{x}{x-1} \ln x \right]. \end{aligned} \quad (3.7)$$

Neglecting the strange quark mass, the effective Hamiltonian (3.1) leads to the following matrix element for the inclusive $b \rightarrow s \tau^+ \tau^-$ decay,

$$\begin{aligned}\mathcal{M} = & \frac{\alpha_{em} G_F}{2\sqrt{2}\pi} V_{tb} V_{ts}^* \left\{ -2C_7^{eff} \frac{m_b}{p^2} \bar{s}i\sigma_{\mu\nu} p_\nu (1 + \gamma_5) b \right. \\ & + C_8^{eff} \bar{s}\gamma_\mu (1 - \gamma_5) b\bar{\tau}\gamma_\mu \tau + C_9 \bar{s}\gamma_\mu (1 - \gamma_5) b\bar{\tau}\gamma_\mu \gamma_5 \tau \\ & \left. + C_{Q_1} \bar{s}(1 + \gamma_5) b\bar{\tau}\tau + C_{Q_2} \bar{s}(1 + \gamma_5) b\bar{\tau}\gamma_5 \tau \right\}.\end{aligned}\quad (3.8)$$

The Wilson coefficients C_i , C_{Q_i} are to be evaluated from m_W down to the lower scale of about m_b by using the renormalization group equation (RGE). When evolving down to b quark scale, the operators $\mathcal{O}_{1,2}$ and \mathcal{Q}_3 can mix with \mathcal{O}_i , ($i = 7, 8$); however, they can be included in an “effective” $\mathcal{O}_{7,8}$ because of their same structures contributing to the $b \rightarrow s\tau^+\tau^-$ matrix element. At leading order, the Wilson coefficients are [3–5]

$$C_7^{eff}(m_b) = \eta^{-16/23} \left\{ C_7(m_W) - \left[\frac{58}{135} (\eta^{10/23} - 1) + \frac{29}{189} (\eta^{28/23} - 1) \right] C_2(m_W) - 0.012 C_{Q_3}(m_W) \right\}, \quad (3.9)$$

$$\begin{aligned}C_8^{eff}(m_b) = & C_8(m_W) + \frac{4\pi}{\alpha_s(m_b)} \left[\frac{4}{33} (\eta^{-11/23} - 1) + \frac{8}{87} (1 - \eta^{-29/23}) \right] \\ & + \left\{ g\left(\frac{m_c}{m_b}, \frac{p^2}{m_b^2}\right) - \frac{3\pi}{\alpha_{em}^2} \kappa \sum_{V_i=\Psi', \Psi'', \dots} \frac{m_{V_i} \Gamma(V_i \rightarrow \tau^+\tau^-)}{m_{V_i}^2 - p^2 - im_{V_i} \Gamma_{V_i}} \right\} [3C_1(m_b) + C_2(m_b)],\end{aligned}\quad (3.10)$$

$$C_9(m_b) = C_9(m_W), \quad (3.11)$$

$$C_{Q_i}(m_b) = \eta^{-\gamma_Q/\beta_0} C_{Q_i}(m_W). \quad (3.12)$$

Here p is the momentum transfer, and

$$C_{Q_3}(m_W) = \frac{m_b e^2}{m_\tau g^2} [C_{Q_1}(m_W) + C_{Q_2}(m_W)] \quad (3.13)$$

where g is the strong coupling constant, $\gamma_Q = -4$ is the anomalous dimension of $\bar{s}Rb$, $\beta_0 = 11 - 2n_f/3$, $\eta = \alpha_s(m_b)/\alpha_s(m_W)$, $C_2(m_W) = 1$ and $C_{1,2}(m_b) = (\eta^{-6/23} \mp \eta^{12/23})/2$. $g(m_c^2/m_b^2, s)$ in Eqs. (3.10) arises from the one-loop matrix elements of the four-quark operators, and

$$g(x, y) = -\frac{4}{9} \ln x + \frac{8}{27} + \frac{16x}{9y} - \frac{4}{9} \left(1 + \frac{2x}{y}\right) \left|1 - \frac{4x}{y}\right|^{1/2} \begin{cases} \ln z + i\pi & \text{for } 4x/y < 1 \\ 2 \arctan \frac{1}{\sqrt{4x/y-1}} & \text{for } 4x/y > 1 \end{cases} \quad (3.14)$$

where

$$z \equiv Z(x, y) = \frac{1 + \sqrt{1 - \frac{4x}{y}}}{1 - \sqrt{1 - \frac{4x}{y}}}. \quad (3.15)$$

The second term in brace in Eq. (3.10) estimates the long-distance contribution from the intermediate Ψ', Ψ'', \dots [3]. The phenomenological parameter κ is taken as 2.3 [19] in our numeral calculations.

After a straightforward calculation, we obtain the invariant dilepton mass distribution [4]

$$\frac{d\Gamma(B \rightarrow X_s \tau^+ \tau^-)}{ds} = Br(B \rightarrow X_c \ell \nu) \frac{\alpha_{em}^2}{4\pi^2} \left| \frac{V_{tb} V_{ts}^*}{V_{cb}} \right|^2 f^{-1}(m_c/m_b) (1-s)^2 (1 - \frac{4r}{s})^{1/2} D(s) \quad (3.16)$$

with

$$\begin{aligned}D(s) = & 4|C_7^{eff}|^2 \left(1 + \frac{2r}{s}\right) \left(1 + \frac{2}{s}\right) + |C_8^{eff}|^2 \left(1 + \frac{2r}{s}\right) (1 + 2s) + |C_9|^2 \left(1 - 8r + 2s + \frac{2r}{s}\right) \\ & + 12Re(C_7^{eff} C_8^{eff*}) \left(1 + \frac{2r}{s}\right) + \frac{3}{2} |C_{Q_1}|^2 (s - 4r) + \frac{3}{2} |C_{Q_2}|^2 s + 6Re(C_9 C_{Q_2}^*) r^{1/2}.\end{aligned}\quad (3.17)$$

Here $s = p^2/m_b^2$, $r = m_c^2/m_b^2$ and $f(x) = 1 - 8x^2 + 8x^6 - x^8 - 24x^4 \ln x$ is the phase-space factor.

The angular information and the forward-backward asymmetry are also sensitive to the details of the new physics. Defining the forward-backward asymmetry as

$$A_{FB}(s) = \frac{\int_0^1 d\cos\theta (d^2\Gamma/dsd\cos\theta) - \int_{-1}^0 d\cos\theta (d^2\Gamma/dsd\cos\theta)}{\int_0^1 d\cos\theta (d^2\Gamma/dsd\cos\theta) + \int_{-1}^0 d\cos\theta (d^2\Gamma/dsd\cos\theta)} \quad (3.18)$$

where θ is the angle between the momentum of B-meson and τ^+ in the center of mass frame of the dilepton, we obtain

$$A_{FB} = \frac{6(1-4r/s)^{1/2}}{D(s)} \text{Re}(2C_7^{\text{eff}}C_9^* + C_8^{\text{eff}}C_9^*s + 2C_7^{\text{eff}}C_{Q_2}^*r^{1/2} + C_8^{\text{eff}}C_{Q_1}^*r^{1/2}). \quad (3.19)$$

IV. $B_s \rightarrow \tau^+\tau^-\gamma$ IN TECHNICOLOR MODEL WITH SCALARS

Now let us turn to rare radiative decay $B_s \rightarrow \tau^+\tau^-\gamma$. The exclusive decay can be obtained from the inclusive decay $b \rightarrow s\tau^+\tau^-\gamma$, and further, from $b \rightarrow s\tau^+\tau^-$. To achieve this, it is necessary to attach photon to any charged internal and external lines in the Feynman diagrams of $b \rightarrow s\tau^+\tau^-$. As pointed out in Ref. [9], contributions coming from the attachment of photon to any charged internal line are strongly suppressed and we can neglect them safely. However, since the mass of τ -lepton is not much smaller than that of B_s -meson, in $B_s \rightarrow \tau^+\tau^-\gamma$ decay, the contributions of the diagrams with photon radiating from final leptons are comparable with those from initial quarks. When a photon is attached to the initial quark lines, the corresponding matrix element for the $B \rightarrow \tau^+\tau^-\gamma$ decay can be written as

$$\begin{aligned} \mathcal{M}_1 = \frac{\alpha_{em}^{3/2} G_F}{\sqrt{2\pi}} V_{tb} V_{ts}^* \{ & [A \varepsilon_{\mu\alpha\beta\sigma} \epsilon_\alpha^* p_\beta q_\sigma + iB(\epsilon_\mu^*(pq) - (\epsilon^* p)q_\mu)] \bar{\tau} \gamma_\mu \tau \\ & + [C \varepsilon_{\mu\alpha\beta\sigma} \epsilon_\alpha^* p_\beta q_\sigma + iD(\epsilon_\mu^*(pq) - (\epsilon^* p)q_\mu)] \bar{\tau} \gamma_\mu \gamma_5 \tau \}, \end{aligned} \quad (4.1)$$

where

$$\begin{aligned} A &= \frac{1}{m_{B_s}^2} [C_8^{\text{eff}} g_1(p^2) - 2C_7 \frac{m_b}{p^2} g_2(p^2)], \\ B &= \frac{1}{m_{B_s}^2} [C_8^{\text{eff}} f_1(p^2) - 2C_7 \frac{m_b}{p^2} f_2(p^2)], \\ C &= \frac{C_9}{m_{B_s}^2} g_1(p^2), \\ D &= \frac{C_9}{m_{B_s}^2} f_1(p^2). \end{aligned} \quad (4.2)$$

In obtaining Eq. (4.1) we have used

$$\langle \gamma | \bar{s} \gamma_\mu (1 \pm \gamma_5) | B_s \rangle = \frac{e}{m_{B_s}^2} \{ \varepsilon_{\mu\alpha\beta\sigma} \epsilon_\alpha^* p_\beta q_\sigma g_1(p^2) \mp i[(\epsilon_\mu^*(pq) - (\epsilon^* p)q_\mu)] f_1(p^2) \}, \quad (4.3)$$

$$\langle \gamma | \bar{s} i \sigma_{\mu\nu} p_\nu (1 \pm \gamma_5) b | B_s \rangle = \frac{e}{m_{B_s}^2} \{ \varepsilon_{\mu\alpha\beta\sigma} \epsilon_\alpha^* p_\beta q_\sigma g_2(p^2) \pm i[(\epsilon_\mu^*(pq) - (\epsilon^* p)q_\mu)] f_2(p^2) \}, \quad (4.4)$$

and

$$\langle \gamma | \bar{s} (1 \pm \gamma_5) | B_s \rangle = 0. \quad (4.5)$$

Here ϵ_μ and q_μ are the four vector polarization and momentum of photon, respectively. g_i , f_i are form factors [8,20]. Eq. (4.5) can be obtained by multiplying p_μ in both sides of Eq. (4.4) and using the equations of motion. From Eq. (4.5) one can see that the neutral scalars do not contribute to the matrix element \mathcal{M}_1 .

When a photon is radiated from the final τ -leptons, the situation is different. Using the expressions

$$\begin{aligned} \langle 0 | \bar{s} b | B_s \rangle &= 0, \\ \langle 0 | \bar{s} \sigma_{\mu\nu} (1 + \gamma_5) b | B_s \rangle &= 0, \\ \langle 0 | \bar{s} \gamma_\mu \gamma_5 | B_s \rangle &= -i f_{B_s} P_{B_s \mu} \end{aligned} \quad (4.6)$$

and the conservation of the vector current, one finds that the operators $\mathcal{Q}_{1,2}$ and \mathcal{O}_9 give contribution to this Bremsstrahlung part. The corresponding matrix is given by [10]

$$\begin{aligned} \mathcal{M}_2 = \frac{\alpha_{em}^{3/2} G_F}{\sqrt{2\pi}} V_{tb} V_{ts}^* i 2m_\tau f_{B_s} \{ & (C_9 + \frac{m_{B_s}^2}{2m_\tau m_b} C_{Q_2}) \bar{\tau} [\frac{\not{e} \not{P}_{B_s}}{2p_1 q} - \frac{\not{P}_{B_s} \not{e}}{2p_2 q}] \gamma_5 \tau \\ & + \frac{m_{B_s}^2}{2m_\tau m_b} C_{Q_1} [2m_\tau (\frac{1}{2p_1 q} + \frac{1}{2p_2 q}) \bar{\tau} \not{e} \tau + \bar{\tau} (\frac{\not{e} \not{P}_{B_s}}{2p_1 q} - \frac{\not{P}_{B_s} \not{e}}{2p_2 q}) \gamma_5 \tau] \} \}. \end{aligned} \quad (4.7)$$

Here P_{B_s} , f_{B_s} are the momentum and the decay constant of the B_s meson.

Finally, the total matrix element for the $B_s \rightarrow \tau^+\tau^-\gamma$ decay is obtained as a sum of the \mathcal{M}_1 and \mathcal{M}_2 . After summing over the spins of the τ -leptons and polarization of the photon, we get the square of the matrix element as

$$|\mathcal{M}|^2 = |\mathcal{M}_1|^2 + |\mathcal{M}_2|^2 + 2\text{Re}(\mathcal{M}_1\mathcal{M}_2^*) \quad (4.8)$$

with¹

$$\begin{aligned} |\mathcal{M}_1|^2 &= 4\left|\frac{\alpha_{em}^{3/2}G_F}{\sqrt{2\pi}}V_{tb}V_{ts}^*\right|^2 \left\{ [|A|^2 + |B|^2][p^2((p_1q)^2 + (p_2q)^2) + 2m_\tau^2(pq)^2] \right. \\ &\quad \left. + [|C|^2 + |D|^2][p^2((p_1q)^2 + (p_2q)^2) - 2m_\tau^2(pq)^2] \right. \\ &\quad \left. + 2\text{Re}(B^*C + A^*D)p^2((p_1q)^2 - (p_2q)^2) \right\}, \end{aligned} \quad (4.9)$$

$$\begin{aligned} 2\text{Re}(\mathcal{M}_1\mathcal{M}_2^*) &= -16\left|\frac{\alpha_{em}^{3/2}G_F}{\sqrt{2\pi}}V_{tb}V_{ts}^*\right|^2 m_\tau^2 f_{B_s}(pq)^2 \left\{ |C_9 + \frac{m_{B_s}^2 C_{Q_2}}{2m_\tau m_b}| \left[\text{Re}(A)\frac{(p_1q + p_2q)}{(p_1q)(p_2q)} \right. \right. \\ &\quad \left. \left. - \text{Re}(D)\frac{(p_1q - p_2q)}{(p_1q)(p_2q)} \right] + \text{Re}(B)\left|\frac{m_{B_s}^2 C_{Q_1}}{2m_\tau m_b}\right| \left[\frac{3m_{B_s}^2 + 2m_\tau^2 - 5(pq)}{(p_1q)(p_2q)} - \frac{2p^2}{(pq)^2} \right] \right. \\ &\quad \left. + \text{Re}(C)\left|\frac{m_{B_s}^2 C_{Q_1}}{2m_\tau m_b}\right| \left[\frac{(p_1q - p_2q)}{(p_1q)(p_2q)}(1 + \frac{2p^2}{(pq)^2}) \right] \right\}, \end{aligned} \quad (4.10)$$

$$\begin{aligned} |\mathcal{M}_2|^2 &= -8\left|\frac{\alpha_{em}^{3/2}G_F}{\sqrt{2\pi}}V_{tb}V_{ts}^*\right|^2 m_\tau^2 f_{B_s}^2 \left\{ |C_9 + \frac{m_{B_s}^2 C_{Q_2}}{2m_\tau m_b}|^2 \left[\frac{m_\tau^2 m_{B_s}^2 (pq)^2}{(p_1q)^2 (p_2q)^2} - \frac{m_{B_s}^2 p^2 + 2(pq)^2}{(p_1q)(p_2q)} \right] \right. \\ &\quad \left. - \left|\frac{m_{B_s}^2 C_{Q_1}}{2m_\tau m_b}\right|^2 \left[\frac{m_\tau^2 (m_{B_s}^2 - 4m_\tau^2) (pq)^2}{(p_1q)^2 (p_2q)^2} - \frac{(m_{B_s}^2 - 4m_\tau^2) p^2 + 2(pq)^2}{(p_1q)(p_2q)} \right] \right\}. \end{aligned} \quad (4.11)$$

Here p_1 , p_2 are momenta of the final τ -leptons. It is obvious that the quantity $|\mathcal{M}|^2$ depends only on the scalar products of the momenta of the external particles.

In the rest frame of the B_s , the photon energy E_γ and the lepton energy E_1 are restricted by

$$\begin{aligned} 0 \leq E_\gamma &\leq \frac{m_{B_s}^2 - 4m_\tau^2}{2m_{B_s}}, \\ \frac{m_{B_s} - E_\gamma}{2} - \frac{E_\gamma}{2} \sqrt{1 - \frac{4m_\tau^2}{m_{B_s}^2 - 2m_{B_s}E_\gamma}} &\leq E_1 \leq \frac{m_{B_s} - E_\gamma}{2} + \frac{E_\gamma}{2} \sqrt{1 - \frac{4m_\tau^2}{m_{B_s}^2 - 2m_{B_s}E_\gamma}}. \end{aligned} \quad (4.12)$$

However, in $|\mathcal{M}_2|^2$ it appears an infrared divergence, which originates in the Bremsstrahlung processes when photon is soft and in this case, the $B_s \rightarrow \tau^+\tau^-\gamma$ can not be distinguished from $B_s \rightarrow \tau^+\tau^-$. Therefore, both processes must be considered together in order to cancel the infrared divergence. Taking the fact that the infrared singular terms in $|\mathcal{M}_2|^2$ exactly cancel the $O(\alpha_{em})$ virtual correction in $B_s \rightarrow \tau^+\tau^-$ amplitude in account [9], we follow Ref. [9] and consider the photon in $B_s \rightarrow \tau^+\tau^-\gamma$ as a hard photon and impose a cut on the photon energy E_γ , which correspond to the radiated photon can be detected in the experiments. This cut requires $E_\gamma \geq \delta m_{B_s}/2$ with $\delta = 0.02$.

After integrating over the phase space and the lepton energy E_1 , we express the decay rate as

$$\begin{aligned} \Gamma &= \left|\frac{\alpha_{em}^{3/2}G_F}{2\sqrt{2\pi}}V_{tb}V_{ts}^*\right|^2 \frac{m_{B_s}^5}{(2\pi)^3} \left\{ \frac{m_{B_s}^2}{12} \int_{4\hat{r}}^{1-\delta} (1-\hat{s})^3 d\hat{s} \sqrt{1 - \frac{4\hat{r}}{\hat{s}}} [(|A|^2 + |B|^2)(\hat{s} + 2\hat{r}) \right. \\ &\quad \left. + (|C|^2 + |D|^2)(\hat{s} - 4\hat{r})] - 2f_{B_s}|C_9 + \frac{m_{B_s}^2 C_{Q_2}}{2m_\tau m_b}| \hat{r} \int_{4\hat{r}}^{1-\delta} (1-\hat{s})^2 d\hat{s} \text{Re}(A) \ln \hat{z} \right\} \end{aligned}$$

¹There are some errors in Eqs. (15) and (17) in Ref. [10]. We believe the expressions of $C_{Q_1}^H(m_W)$ and $C_{Q_2}^H(m_W)$ are not correct in Two-Higgs-Doublet model I.

$$\begin{aligned}
& -2f_{B_s} \left| \frac{m_{B_s}^2 C_{Q_1}}{2m_\tau m_b} \right| \hat{r} \int_{4\hat{r}}^{1-\delta} (1-\hat{s}) d\hat{s} \text{Re}(B) \left[(1+4\hat{r}-5\hat{s}) \ln \hat{z} + x \sqrt{1-\frac{4\hat{r}}{\hat{s}}} \right] \\
& - \frac{4f_{B_s}^2}{m_{B_s}^2} \left| C_9 + \frac{m_{B_s}^2 C_{Q_2}}{2m_\tau m_b} \right|^2 \hat{r} \int_{4\hat{r}}^{1-\delta} d\hat{s} \left[(1+\hat{s} + \frac{4\hat{r}-2}{1-\hat{s}}) \ln \hat{z} + \frac{2\hat{s}}{1-\hat{s}} \sqrt{1-\frac{4\hat{r}}{\hat{s}}} \right] \\
& + f_{B_s}^2 \left| \frac{C_{Q_1}}{m_b} \right|^2 \int_{4\hat{r}}^{1-\delta} d\hat{s} \left[(1-8\hat{r}+\hat{s} - \frac{2-10\hat{r}+8\hat{r}^2}{1-\hat{s}}) \ln \hat{z} + \frac{2(1-4\hat{r})\hat{s}}{1-\hat{s}} \sqrt{1-\frac{4\hat{r}}{\hat{s}}} \right] \}
\end{aligned} \tag{4.13}$$

where $\hat{s} = p^2/m_{B_s}^2$, $\hat{r} = m_\tau^2/m_{B_s}^2$ and $\hat{z} \equiv Z(\hat{r}, \hat{s})$.

V. NUMERICAL RESULTS AND DISCUSSIONS

In this section we give some numerical results and discussions. For reference, we present our SM predictions²

$$\begin{aligned}
Br(B \rightarrow X_s \tau^+ \tau^-) &= 2.60 \times 10^{-6}, \\
Br(B_s \rightarrow \tau^+ \tau^- \gamma) &= 5.19 \times 10^{-8}.
\end{aligned} \tag{5.1}$$

These values are obtained for the fixed input parameters listed in Table I [21] and the QCD coupling constant $\alpha_s(m_b) = 0.218$ which are calculated via

$$\alpha_s(\mu) = \frac{\alpha_s(m_Z)}{1 - \beta_0 \frac{\alpha_s(m_Z)}{2\pi} \ln \frac{m_Z}{\mu}}. \tag{5.2}$$

with $\alpha_s(m_Z) = 0.119$ [21] and $m_Z = 91.19 \text{ GeV}$.

Table I. The value of the input parameters used in the numerical calculations (mass and decay constant in unit GeV).

m_t	m_c	m_b	m_τ	m_{B_s}	m_W
176	1.4	4.8	1.78	5.26	80.448
f_{B_s} [22]	$ V_{tb}V_{ts}^* $	$ V_{tb}V_{ts}^*/V_{cb} ^2$	α_{em}^{-1}	$\tau(B_s)$	$\sin^2 \theta_W$
0.14	0.045	0.95	137	$1.64 \times 10^{-12} \text{ s}$	0.2325

In addition, we use the masses, decay widths and branching rates of J/Ψ family in Ref. [21], the normalized factor, branching rate $Br(B \rightarrow X_c \ell \nu) = 10.2\%$, and take the dipole forms of the form-factors given by Ref [20]

$$\begin{aligned}
g_1(p^2) &= \frac{1 \text{ GeV}}{(1-p^2/5.6^2)^2}, & g_2(p^2) &= \frac{3.74 \text{ GeV}}{(1-p^2/40.5)^2}, \\
f_1(p^2) &= \frac{0.8 \text{ GeV}}{(1-p^2/6.5^2)^2}, & f_2(p^2) &= \frac{0.68 \text{ GeV}}{(1-p^2/30)^2}.
\end{aligned} \tag{5.3}$$

As mentioned in Sec. II, in limit (i) and (ii) there are only two independent parameters f/f' and m_{π_p} in technicolor model with scalars. We use the limits on the mass of the Higgs boson in the SM and 2HDM to constrain the masses of the scalars π_p and σ . There are general reasons to believe that the mass of the SM Higgs boson is less than the order of 1 TeV. The new lower bounds $m_H > 107.7 \text{ GeV}$ are given by the LEP Higgs working group [21]³. In this work,

²Our formula for $Br(B_s \rightarrow \tau^+ \tau^-)$ is the same as given in Ref. [9], but different from their result. In fact, the Bremsstrahlung part is 3.98×10^{-8} for $\delta = 0.02$.

³Very recently, ALEPH [23] and L3 [24] updated their results, claiming that a 3σ excess of events above background which are compatible a SM Higgs boson with a mass near 114 GeV; however, as pointed out in Ref. [23], more data, or results from other experiments are needed to determine whether their observations are the result of a statistical fluctuation or the first sign of direct production of the Higgs boson.

we simply take $107.7 < m_\sigma < 1000 \text{ GeV}$. The mass of physical scalar π_p is constrained by the limits on m_σ and Eq. (3.5). Since we are only interested in the region with large f/f' limit, i.e., we set f/f' varying 10 to 20 in the allowed parameter space, the constraints mentioned above imply a large m_{π_p} , $330 \leq m_{\pi_p} < 1000 \text{ GeV}$, which is consistent with the lower bound on charged Higgs boson in 2HDMs [21]. Our constraints on parameter space $(f/f', m_{\pi_p})$ are very stringent. From example, for $f/f' = 10$ the value of m_{π_p} is limited in $330 \sim 600 \text{ GeV}$.

Now we present some numerical results in limit (i) and (ii). The branching ratios of $B \rightarrow X_s \tau^+ \tau^-$ and $B_s \rightarrow \tau^+ \tau^- \gamma$ as functions of f/f' are shown in Fig. 3 and Fig. 4. The dependences of the branching ratios on the mass of the charged scalar are given in Fig. 5 and Fig. 6. These results manifest that the branching ratios predicted by the technicolor model have large enhancements (a couple of orders) over those predicted by the SM. In contrast to the decays studied in 2HDM-II [10], the contributions from the charged scalars are not suppressed but enhanced by a factor $(\frac{f}{f'})^2$ when f/f' is large. Therefore, the charged scalars give dominant contributions to the processes.

Further, we find that contributions to $B \rightarrow X_s \tau^+ \tau^-$ from neutral scalars increase the branching ratios; however, these contributions are small and can be neglected safely. For the rare radiative decay $B_s \rightarrow \tau^+ \tau^- \gamma$, the situation is different, the neutral scalars contributions are large enough to be comparable with the SM contributions.

We plot the differential branching ratios of $B \rightarrow X_s \tau^+ \tau^-$ (normalized to $\Gamma(B \rightarrow X_c e \nu_e)$) and $B_s \rightarrow \tau^+ \tau^- \gamma$ as a functions of scaled invariant dilepton mass in Fig. 7 and Fig. 8. The forward-backward asymmetry of $B \rightarrow X_s \tau^+ \tau^-$ is shown in Fig. 9. One can see that differing from the case of $B_s \rightarrow \tau^+ \tau^- \gamma$, whose differential branching ratio always increases with increase of scaled invariant dilepton mass, the differential branching ratio of $B \rightarrow X_s \tau^+ \tau^-$ decay increases rapidly to its maximum and then decreases with bigger \hat{s} . Fig. 9 indicates the significant difference in the forward-backward asymmetry predictions between the SM and technicolor model, especially in the region of large invariant dilepton mass. Since there exist no uncertainties, such as CKM matrix elements, phase-space factor, etc., in calculating the forward-backward asymmetry A_{FB} (see Eq. (3.18)), the measurement of the forward-backward asymmetry will give important clues about the new physics beyond the SM.

In summary, in the framework of technicolor with scalars we have calculated the differential branching ratios and branching ratios of $B \rightarrow X_s \tau^+ \tau^-$ and $B_s \rightarrow \tau^+ \tau^- \gamma$, as well as the forward-backward asymmetry of $B \rightarrow X_s \tau^+ \tau^-$. The contributions from both the neutral and the charged scalars are considered. Changes of the branching ratios with the model parameters f/f' and m_{π_p} are investigated. We found that in large f/f' limit, the branching ratios and forward-backward asymmetry of $B \rightarrow X_s \tau^+ \tau^-$ have large enhancements over those predicted by the SM. Such large enhancements could be detectable in future B-meson factories. Therefore, the sizable enhancements predicted by this technicolor model will either distinguish this model from the SM or make further constraints on model parameter space.

ACKNOWLEDGMENT

We thank C.-H. Chang for discussions and comments. This work is supported in part by a grant of Chinese Academy of Science for Outstanding Young Scholars.

-
- [1] R. Ammar, *et al.*, CLEO Collaboration, Phys. Rev. Lett. **71**, 674 (1993); M. S. Alam *et al.*, CLEO Collaboration, Phys. Rev. Lett. **74**, 2885 (1995).
[2] Y. Grossman, Z. Ligeti, and E. Nardi, Phys. Rev. D **55**, 2768 (1997).
[3] B. Grinstein, R. Springer, and M. B. Wise, Phys. Lett. B **202**, 138 (1988); Nucl. Phys. B **339**, 269 (1990).
[4] Y. B. Dai, C. S. Huang and H. W. Huang, Phys. Lett. B **390**, 257 (1997).
[5] J. L. Hewett, Phys. Rev. D **53**, 4964 (1996).
[6] S. Weinberg, Phys. Rev. D **19**, 1277 (1979); L. Susskind, Phys. Rev. D **20**, 2619 (1979).
[7] S. Dimopoulos and L. Susskind, Nucl. Phys. B **155**, 237 (1979); E. Eichten and K. Lane, Phys. Lett. B **90**, 125 (1980).
[8] G. Buchalla and A. J. Buras, Nucl. Phys. B **400**, 225 (1993); D. Du, C. Liu and D. Zhang, Phys. Lett. B **317**, 179 (1993).
[9] T. M. Aliev, A. ÖZpineci and M. Savci, Phys. Rev. D **55**, 7059 (1997); T. M. Aliev, N. K. Pak and M. Savci, Phys. Lett. B **424**, 175 (1998).
[10] E. O. Ilhan and G. Turan, Phys. Rev. D **61**, 034010 (2000).
[11] E. H. Simmons, Nucl. Phys. B **312**, 253 (1989).

- [12] C. D. Carone and E. H. Simmons, Nucl. Phys. **B397**, 591 (1993); C. D. Carone and H. Georgi, Phys. Rev. **D49**, 1427 (1994).
- [13] M. Neubert, Phys. Rep. **245**, 396 (1994).
- [14] A. Falk, M. Misiak, and M. Muñiz, Nucl. Phys. **B49**, 3367 (1994); A. Falk, M. Luke, and M. Savage, Phys. Rev. D **53**, 2491 (1996); I. Bigi, M. Shifman, N. G. Uraltsev, and A. I. Vainshtein, Phys. Rev. Lett. **71**, 496 (1993); A. V. Manohar and M. B. Wise, Phys. Rev. D **49**, 1310 (1994).
- [15] G. Lu, Z. Xiong and Y. Cao, Nucl. Phys. **B487**, 43 (1997).
- [16] Z. Xiong, H. Chen and L. Lu, Nucl. Phys. **B561**, 3 (1999).
- [17] C. D. Carone and Y. Su, Phys. Lett. B **344**, 2015 (1995).
- [18] Y. Su, Phys. Rev. D **56**, 335 (1997).
- [19] A. Ali and C. Creub, Z. Phys. C **49**, 431 (1991); Phys. Lett. B **259**, 182 (1991); **361**, 146 (1995).
- [20] G. Eilam, I. Halperin and R. R. Mendel, Phys. Lett. B **361**, 137 (1995).
- [21] Particle Physics Group. Eur. Phys. J. C 1998, **15**, 274 (2000).
- [22] V. M. Belyaev *et al.*, Phys. Rev. D **51**, 6177 (1995).
- [23] ALEPH Collaboration, CERN-EP/2000-138. Submitted to Phys. Lett. B
- [24] L3 Collaboration, CERN-EP/2000-140. Submitted to Phys. Lett. B.

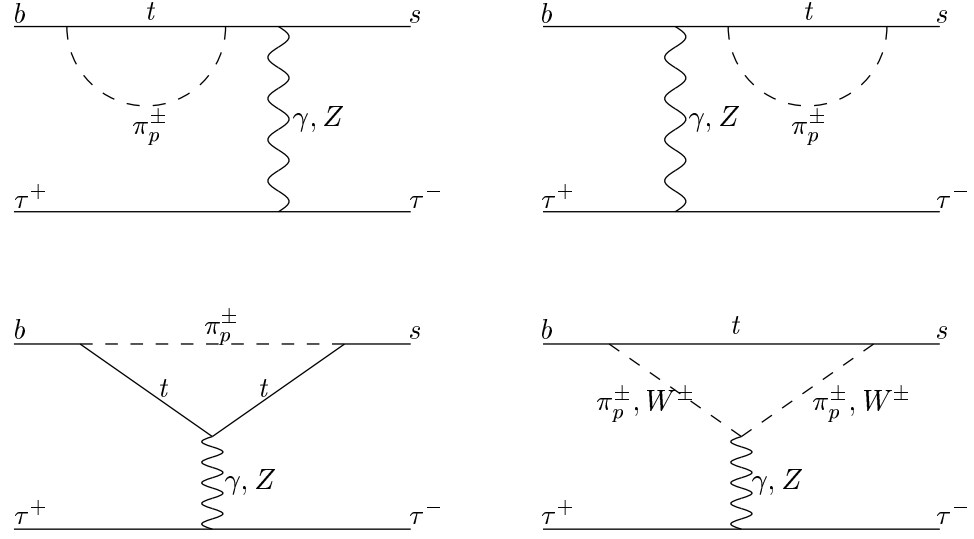


FIG. 1. Feynman diagrams for the charged scalar contributions in technicolor with scalars.

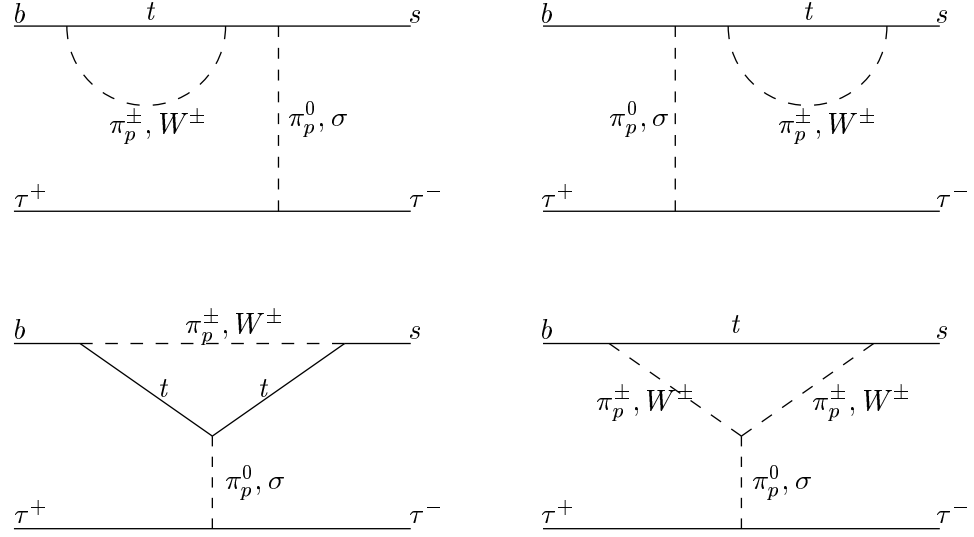


FIG. 2. Feynman diagrams for the additional contributions from the neutral scalars in technicolor with scalars.

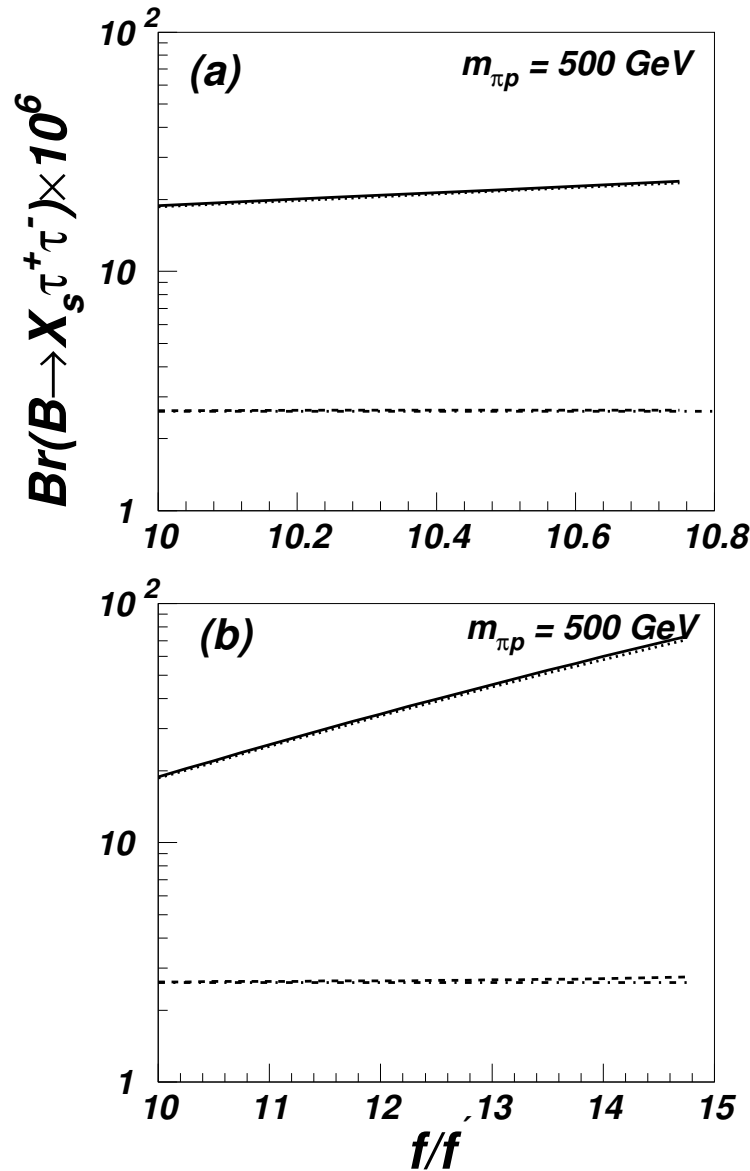


FIG. 3. Branching ratio of $B \rightarrow X_s \tau^+ \tau^-$ as a function of f/f' . (a) and (b) correspond to the technicolor model in limit (i) and (ii), respectively. The dot-dashed line stands for the SM prediction. The dotted (dashed) lines represent the new physics contributions from γ , Z exchange (neutral scalar exchange) diagrams shown in Fig.1 (Fig.2). The solid one is the total values with $m_{\pi p} = 500 \text{ GeV}$.

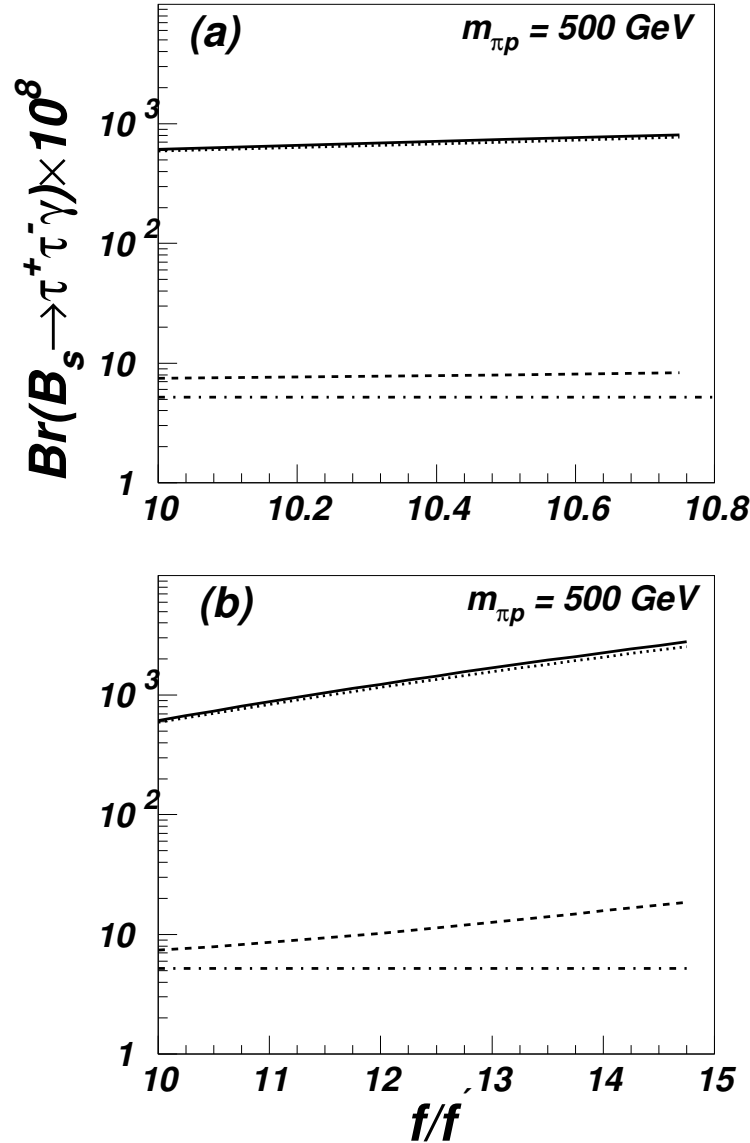


FIG. 4. The same as Fig. 3, but for $B_s \rightarrow \tau^+ \tau^- \gamma$.

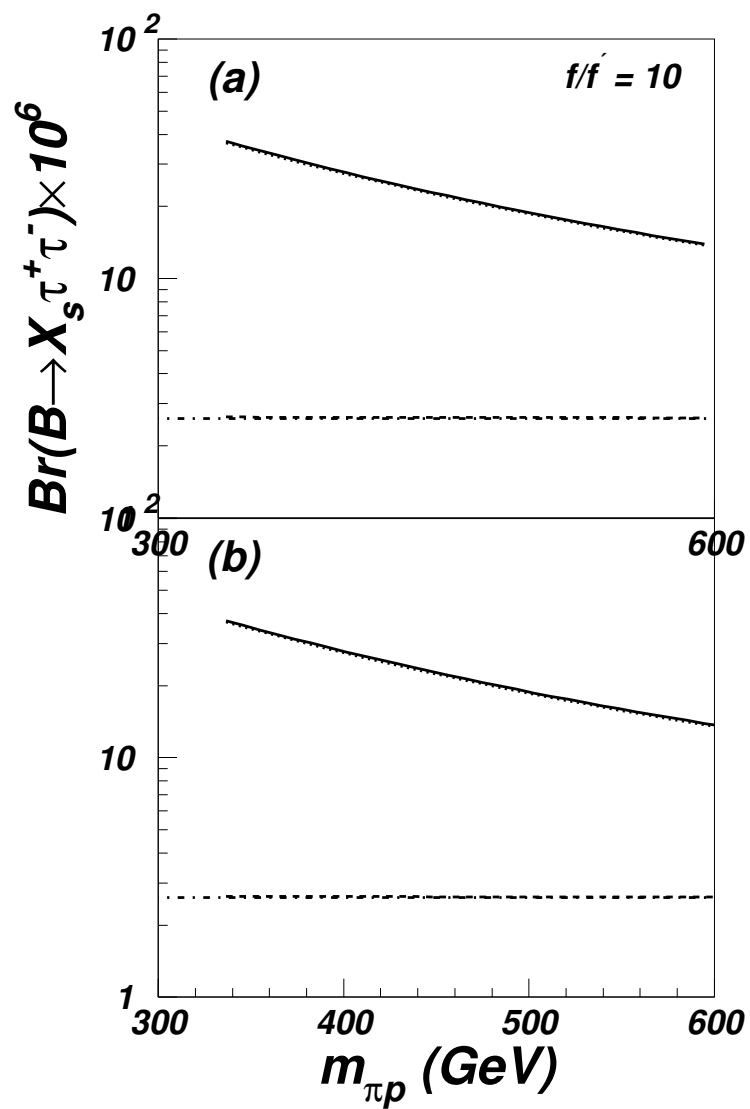


FIG. 5. The same as Fig. 3, but versus $m_{\pi p}$ for $f/f' = 10$.

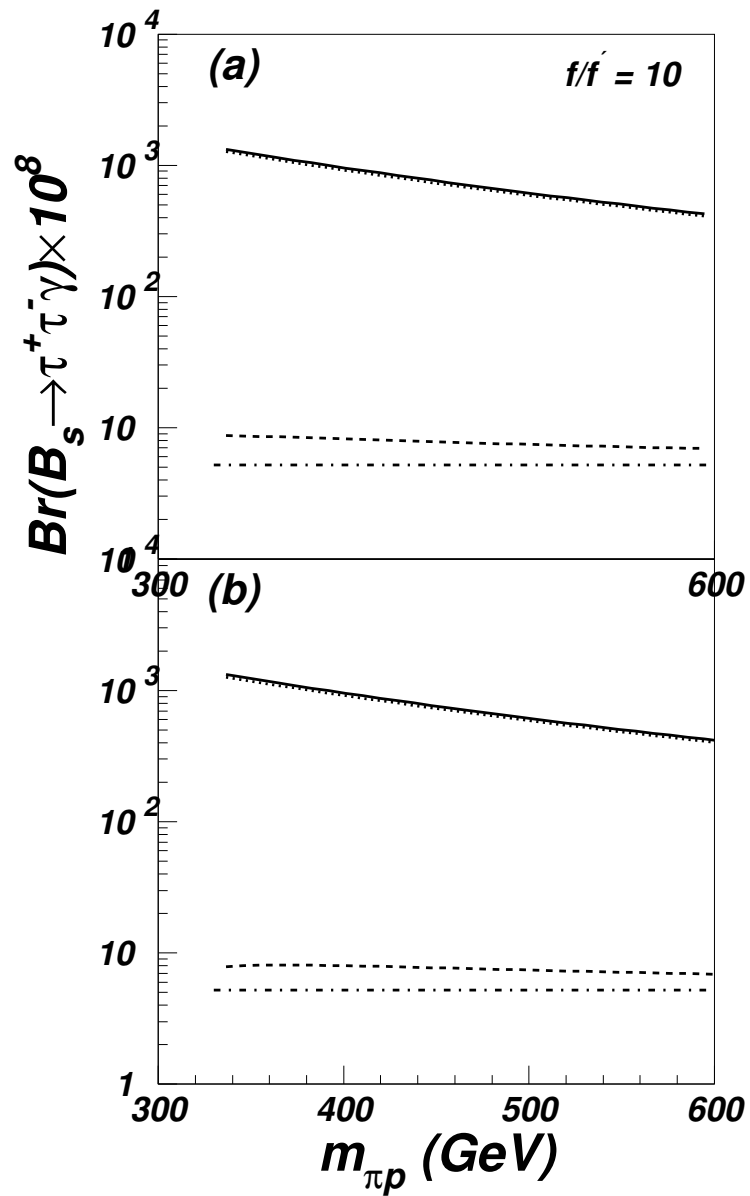


FIG. 6. The same as Fig. 3, but for $B_s \rightarrow \tau^+ \tau^- \gamma$ versus $m_{\pi p}$ with $f/f' = 10$.

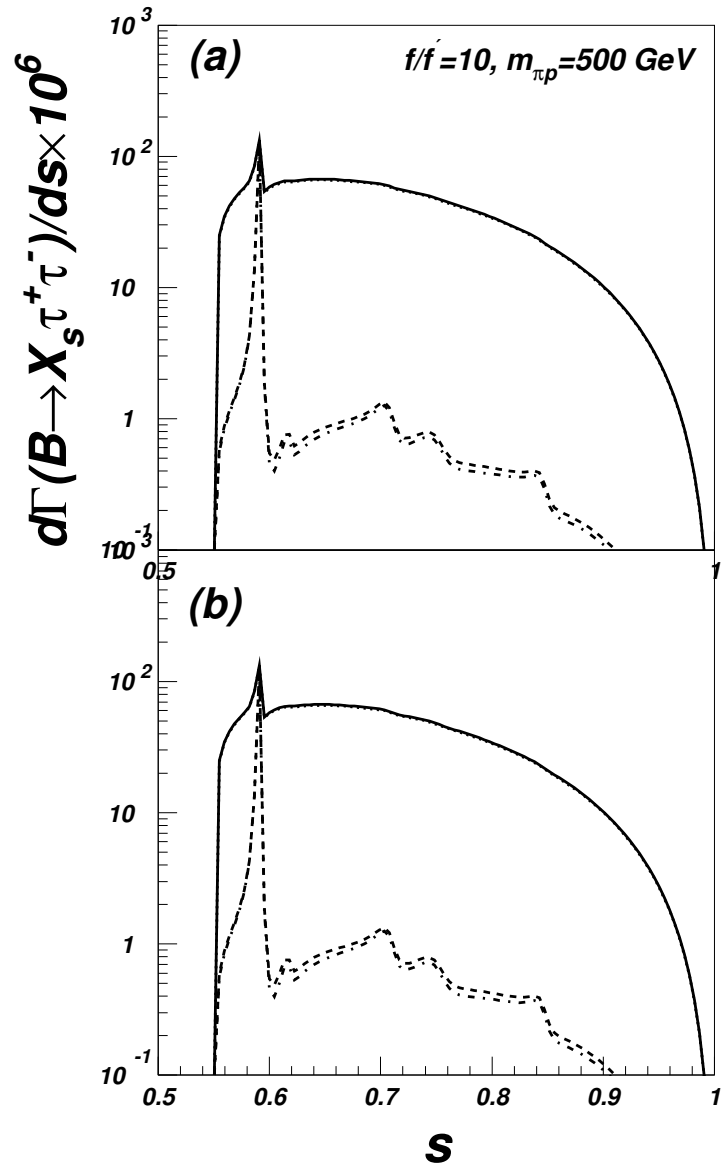


FIG. 7. The same as Fig. 3, but for differential branching ratio versus the invariant dilepton mass s with $f/f' = 10$ and $m_{\pi p} = 500 \text{ GeV}$.

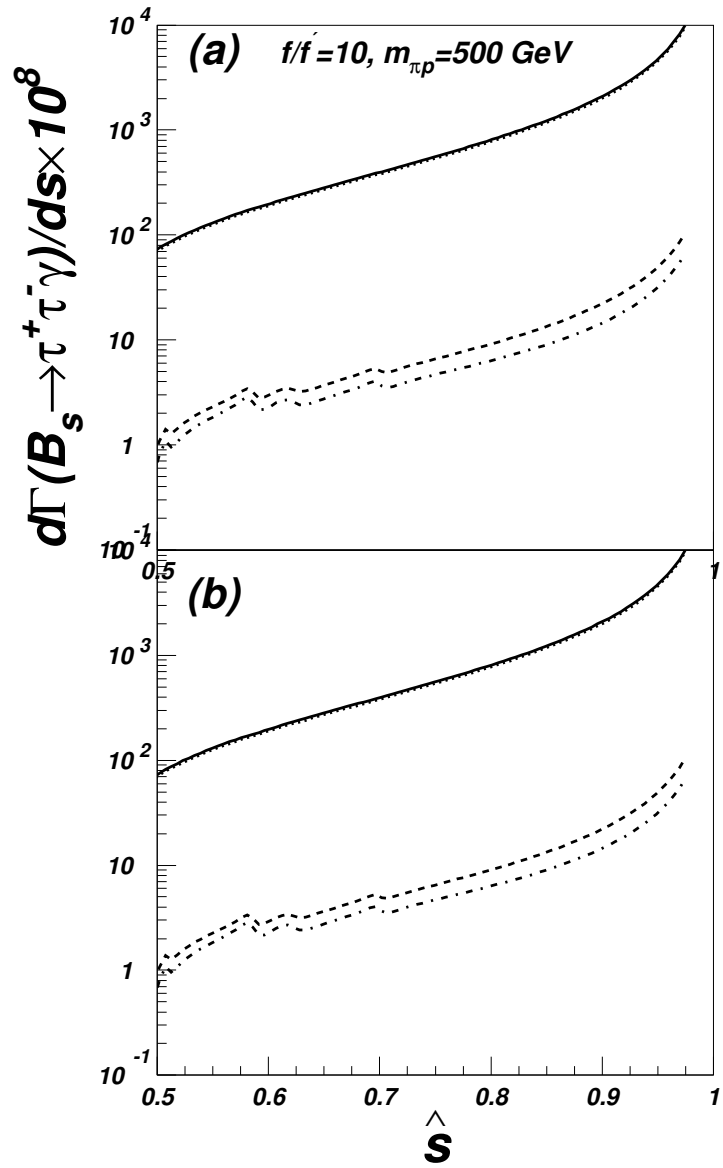


FIG. 8. The same as Fig. 3, but for differential branching ratio of $B_s \rightarrow \tau^+ \tau^- \gamma$ versus \hat{s} with $f/f' = 10$ and $m_{\pi p} = 500 \text{ GeV}$.

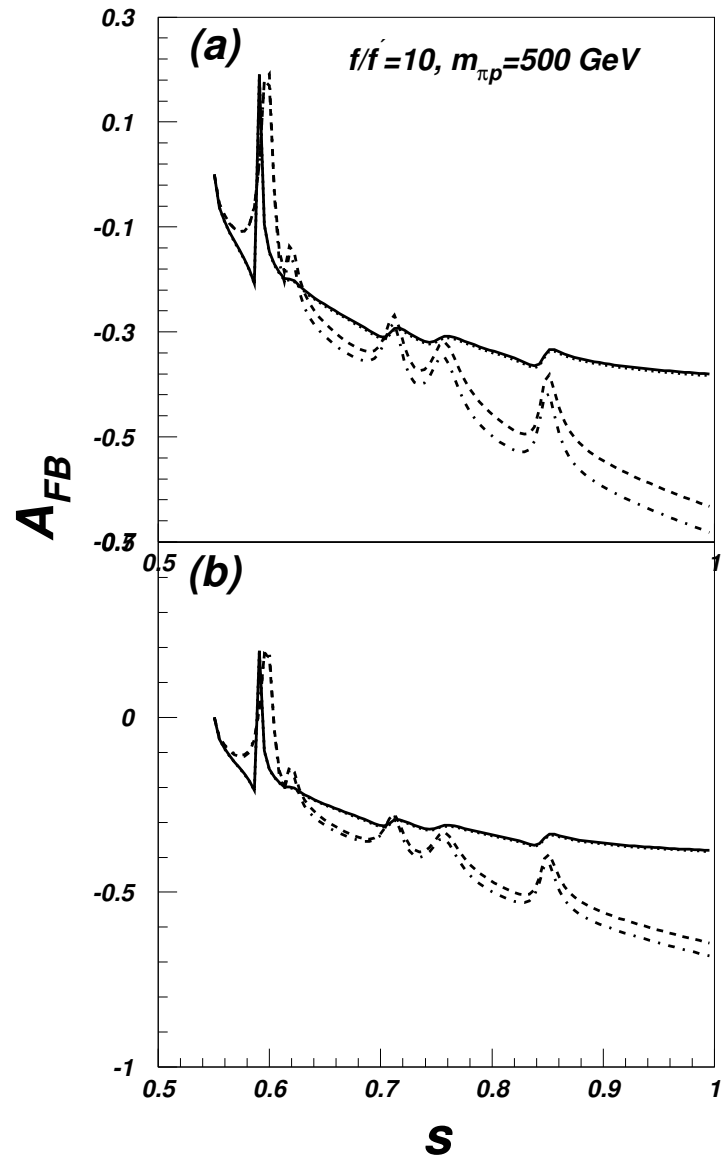


FIG. 9. The same as Fig. 3, but for the forward-backward asymmetry of $B \rightarrow X_s \tau^+ \tau^-$ versus s with $f/f' = 10$ and $m_{\pi_p} = 500 \text{ GeV}$.